Progress In Electromagnetics Research Letters, Vol. 75, 13–18, 2018

Miniature Multiband Antenna for WLAN and X-Band Satellite Communication Applications

Ruixing Zhi, Mengqi Han, Jing Bai, Wenying Wu, and Gui Liu*

Abstract—A novel miniature microstrip-fed multiband antenna for wireless local area network (WLAN) and X-band satellite communication applications is presented in this paper. The proposed antenna consists of two arc-shaped strips, dual inverted L-shaped parasitic stubs, and a partial ground plane. The proposed antenna can excite multi-resonant modes while achieving a compact size of $18 \times 34.5 \times 0.8\,\text{mm}^3$. The measurement results show that $-10\,\text{dB}$ impedance bandwidths are 290 MHz (2.28–2.57 GHz), 1.27 GHz (5.0–6.27 GHz), and 850 MHz (7.11–7.96 GHz), which can cover the entire operation frequencies of WLAN (2.48–2.4835 GHz, 5.15–5.875 GHz) and X-band satellite communication system (7.25–7.75 GHz) applications.

1. INTRODUCTION

With the rapid development of wireless communication technologies, there are increasing demands for portable terminals to operate at many frequency bands. However, it remains a big challenge to accommodate many internal antennas in the limited space of mobile terminals. Therefore, multiband antennas are promising candidates for mobile terminals with many wireless communication services due to the capability of operating in several bands [1–3]. In recent years, a lot of remarkable research efforts have been made to develop multiband antennas [1–10]. A triple-band microstrip antenna consisting of F-shaped slot radiators and a defected ground plane was proposed in [1]. A multiband antenna comprising a circular radiating patch with a pair of rectangular slits and an inverted U-shaped slot was presented in [2]. The multiband antenna reported in [3] employs a reflecting ground plane to achieve high gain. Other techniques have been investigated to obtain multiband characteristics such as two circular rings and one open-ended circular ring [4], cylindrical dielectric resonator [5], and PIN diode switches [6].

Most reported multiband antennas are for WLAN/WiMAX applications [1–6]. Several promising multiband antennas have been reported for applications in GPS/WiMAX/WLAN [7], LTE/GSM/UMTS and WLAN/WiMAX [8], TD-LTE/WLAN/WiMAX [9], and C-band/WLAN/International Telecommunications Union (ITU) [10]. In this paper, a multiband antenna for WLAN (2.4–2.4835 GHz, 5.15–5.875 GHz), and X-band satellite communication (7.25–7.75 GHz) applications is proposed. The presented antenna consists of two arc-shaped strips, dual inverted L-shaped stubs and a partial ground plane. The presented structure and design methodology simplify multiband antenna design. Three operating frequency bands of the proposed antenna can be designed and tuned step by step. The effects of different physical parameters of the proposed antenna are discussed, and measurement results are presented.

Received 18 February 2018, Accepted 24 March 2018, Scheduled 8 April 2018
* Corresponding author: Gui Liu (iitgliu2@gmail.com).
The authors are with the College of Mathematics, Physics & Electronic Information Engineering, Wenzhou University, Wenzhou, Zhejiang 325035, China.

2. ANTENNA DESIGN

The detailed geometrical structure of the proposed multiband antenna is shown in Figure 1. The antenna consists of a 50 Ω microstrip feed line and two arc-shaped strips on the top side of the substrate, and dual inverted L-shaped stubs and a rectangular ground plane on the bottom side of the substrate. The length of arc-shaped strips A and B is set close to quarter-wavelength of the lowest resonant frequency (2.45 GHz) and the highest resonant frequency (7.5 GHz), respectively. Therefore, two separate resonant modes with good impedance bandwidth can be excited. The arc length of arc-shaped strip A and B can be calculated by:

$$L = \frac{\text{rad} \times \pi \times R}{180^\circ} = \frac{c}{f \times 4 \times \sqrt{\frac{\varepsilon_r + 1}{2}}} \tag{1}$$

where rad and R are the angle and radius of arc-shaped strip, respectively. c is the speed of light. ε_r is the relative dielectric of the substrate, and f is the desired resonant frequency. Dual inverted L-shaped parasitic stubs are used to achieve the impedance bandwidth to cover the middle frequency band. The proposed antenna is fabricated on a low-cost FR4 substrate with a relative permittivity of 4.4, height of 0.8 mm, and a loss tangent of 0.02. As depicted in Table 1, the proposed antenna shows relative compact size with a thin substrate and simpler geometry compared to other reported antennas.

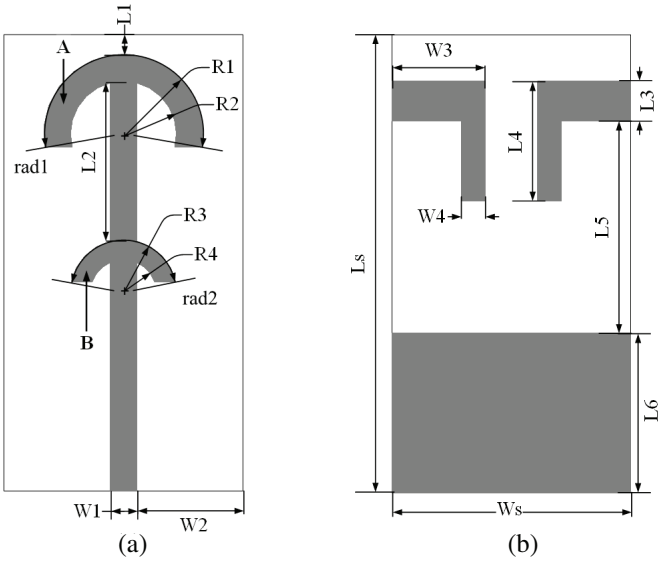

Figure 1. Geometry of the proposed antenna. (a) Top view and (b) Bottom view.

3. RESULTS AND DISCUSSIONS

In order to investigate the operation mechanism of the antenna, several physical parameters of the proposed geometry have been analyzed in the full-wave electromagnetic simulator. Figure 2 shows the reflection coefficients of the proposed antenna with different values of rad1. It shows that the value of rad1 affects all three frequency bands. This is because the arc length of arc-shaped strip A affects the electromagnetic coupling effects between strip A and dual inverted L-shaped stubs on the bottom side of the substrate. By tuning the angle of strip A, the lowest frequency bands can be obtained. Then we can tune other parameters to optimize the middle and highest frequency bands.

Figure 3 shows the simulated reflection coefficient for different values of $L4$ which is one of the parameters of dual inverted L-shaped parasitic stubs. It is noted that the value of $L4$ affects the middle and highest frequency bands a lot while the lowest frequency bands remain almost unchanged. Therefore, the middle frequency bands can be optimized by $L4$. Finally, the value of rad2 can be

Table 1. Performance comparison of the proposed antenna with other reported antennas.

Ref.	Size (mm^3)	Operation Bands (GHz)
[1]	$19 \times 25 \times 1.6$	2.0–2.76, 3.04–4.0, 5.2–6.0
[2]	$25 \times 39 \times 1.59$	2.11–2.69, 3.15–3.89, 5.13–6.23
[3]	$96 \times 73 \times 14$	2.32–3.61, 5.13–6.33
[4]	$25 \times 45 \times 1$	1.93–3.16, 3.4–4.15, 5.15–6.0
[5]	$40 \times 40 \times 1.6$	2.5–2.76, 3.38–3.54, 4.9–5.3, 5.5–5.61, 5.78–5.98
[7]	$22.6 \times 32 \times 0.8$	1.34–1.76, 3.21–3.80, 5.05–6.55
[9]	$24 \times 28.3 \times 1.59$	2.29–2.63, 3.26–3.96, 4.97–6.10
[10]	$23 \times 26 \times 1.6$	4.23–4.32, 5.15–6.12, 7.06–7.29
This work	$18 \times 34.5 \times 0.8$	2.28–2.57, 5.0–6.27, 7.11–7.96

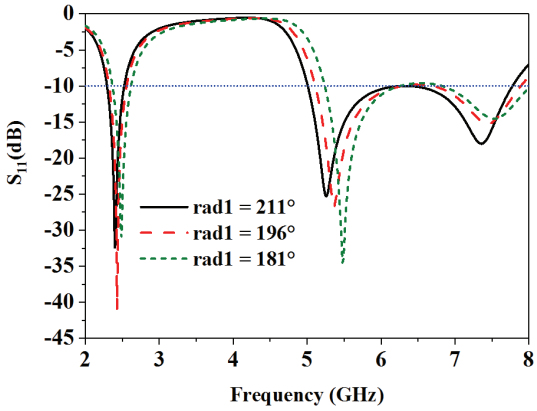

Figure 2. Simulated reflection coefficients for different values of rad1.

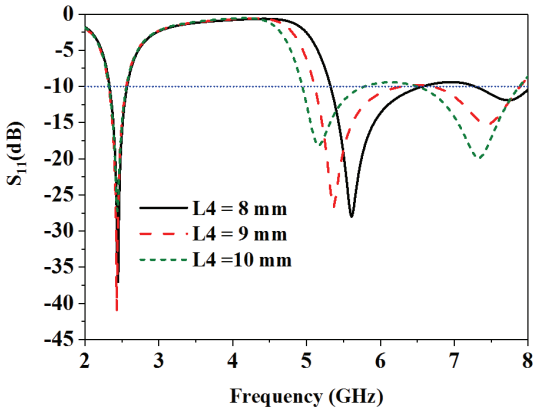

Figure 3. Simulated reflection coefficients for different values of $L4$.

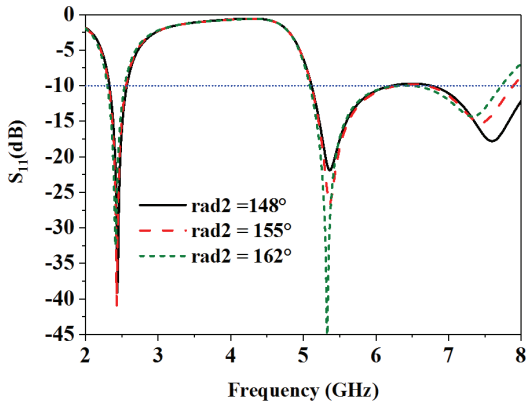

Figure 4. Simulated reflection coefficients for different values of rad2.

optimized to obtain the highest frequency bands while the lowest and middle frequency bands remains almost fixed, as shown in Figure 4.

To further understand the physical mechanism of the proposed antenna, the vector current distributions for three different frequencies are illustrated in Figure 5. Once the length of the conductors is larger than a quarter-wavelength, the vector current distributions may have current nodes where the

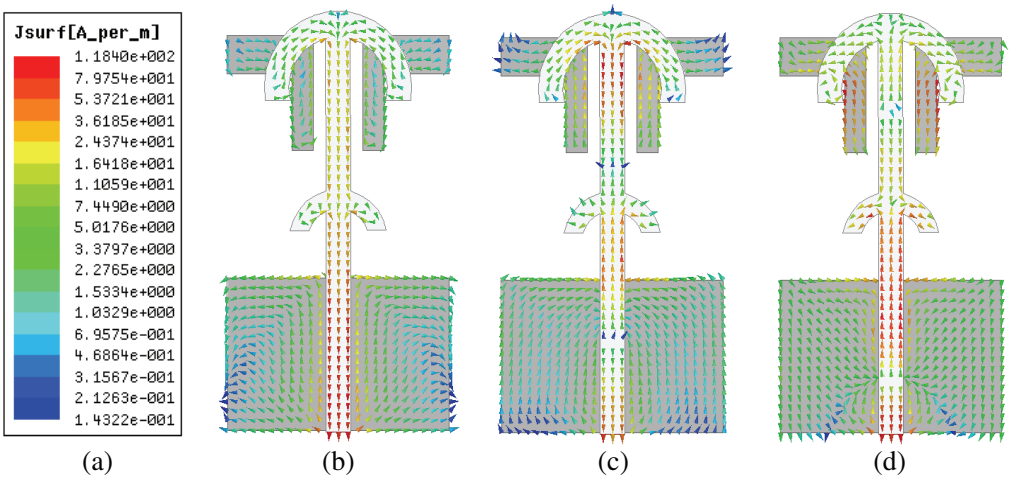

Figure 5. Simulated current distributions at (a) 2.45 GHz (b) 5.5 GHz and (c) 7.5 GHz.

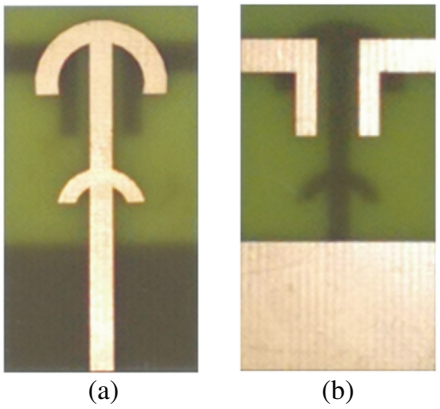

Figure 6. Photograph of the manufactured antenna. (a) Top view and (b) Bottom view.

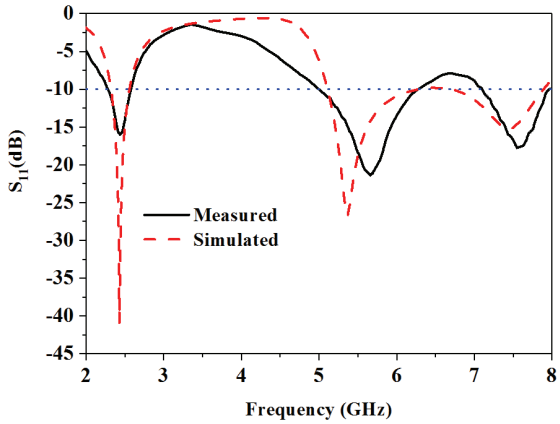

Figure 7. Simulated and measured reflection coefficients.

current vanishes. It is clear that there is no current node on the radiator, and the current mainly follows on strip A and the whole microstrip line at 2.45 GHz, as shown in Figure 5(a). As can be seen from Figure 5(b), the surface current distribution on the dual inverted L-shaped stubs suggests that the value of $L4$ affects the resonance frequency of the middle frequency band. It can be observed that there are two current nodes on the radiator at 5.5 GHz. In Figure 5(c), the current flows along strip B and dual inverted L-shaped stubs, which are responsible for the radiation mechanism at 7.5 GHz.

The optimized final dimensions are $Ws = 18$ mm, $Ls = 34.5$ mm, $W1 = 2$ mm, $L1 = 1.5$ mm, $W2 = 8$ mm, $L2 = 12$ mm, $W3 = 7$ mm, $L3 = 3$ mm, $W4 = 1.75$ mm, $L4 = 9$ mm, $L5 = 16$ mm, $L6 = 12$ mm, $R1 = 6$ mm, $R2 = 4$ mm, $R3 = 4$ mm, $R4 = 2.5$ mm, rad1 = 196°, and rad2 = 155°. To validate the proposed design, a prototype has been fabricated and measured. The photographs of the prototyped antenna are shown in Figure 6. Figure 7 depicts the measured and simulated results of the reflection coefficient of the proposed antenna. The measured reflection coefficients below −10 dB are 2.28–2.57 GHz, 5.0–6.27 GHz and 7.11–7.96 GHz, which can cover WLAN and satellite communication frequency bands. A good agreement between simulated and measured results can be observed in three operation frequency bands.

The normalized measured radiation patterns at 2.45 GHz, 5.5 GHz and 7.5 GHz are shown in Figure 8, respectively. The solid and dash lines stand for co-polarization and cross-polarization, respectively. As shown in Figure 8, the fabricated prototype exhibits nearly dipole-liked radiation patterns in the E-plane and omnidirectional radiation patterns in the H-plane at the respective bands.

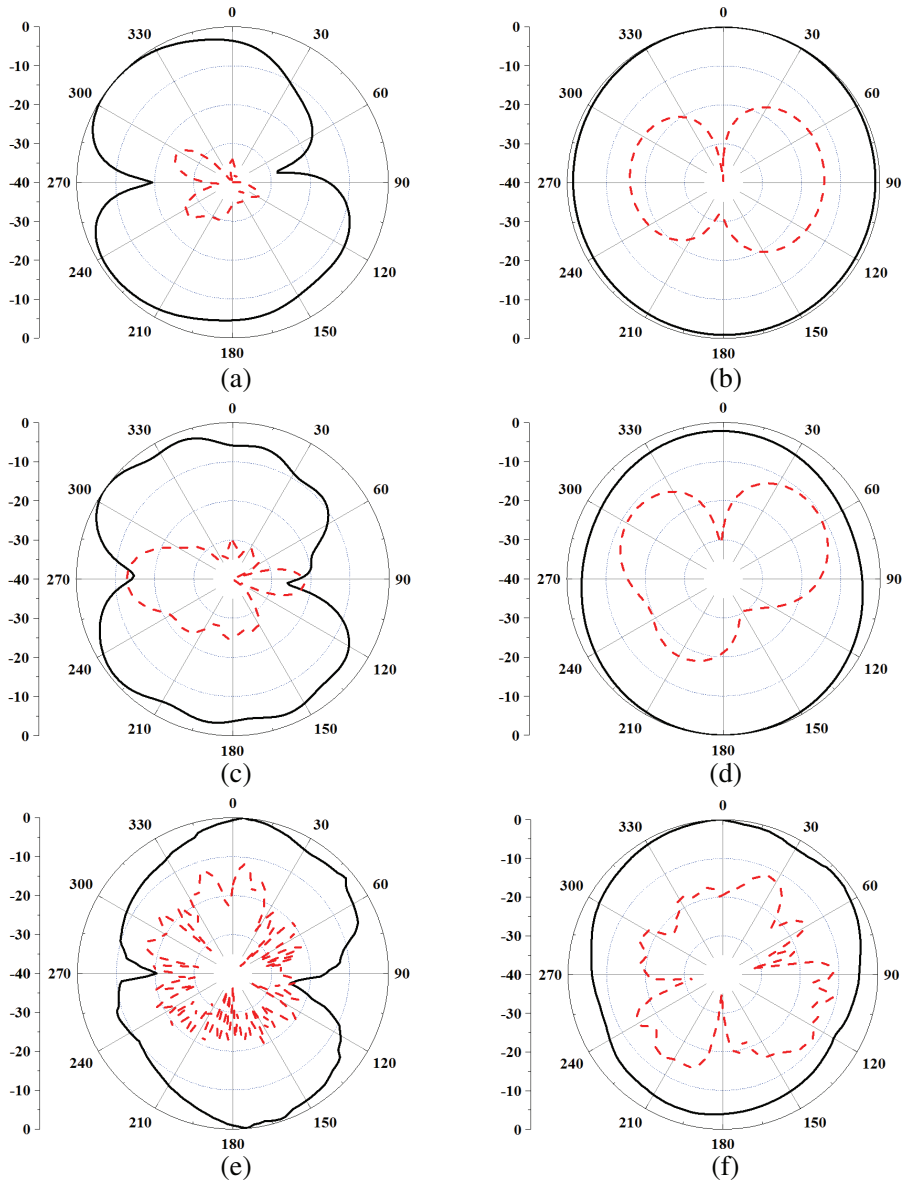

Figure 8. Normalized measured radiation pattern. (a) 2.45 GHz E-plane, (b) 2.45 GHz H-plane, (c) 5.5 GHz E-plane, (d) 5.5 GHz H-plane, (e) 7.5 GHz E-plane, and (f) 7.5 GHz H-plane.

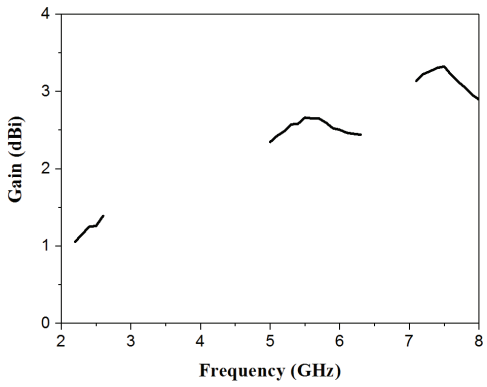

Figure 9. Measured peak gain.

The radiation patterns at the higher frequency bands are deteriorated due to the soldering effects of the SMA connector. Figure 9 shows the measured peak gains of the proposed antenna at three desired operation frequency bands.

4. CONCLUSION

A novel miniature multiband antenna for WLAN and X-band satellite communication applications is presented. The multiband behavior has been achieved due to two arc-shaped strips on the top side of the substrate and dual inverted L-shape stubs on the bottom side of the substrate. The bandwidth of three desired frequency bands can be optimized by some physical parameters. The simulation and measurement results are in good agreement, which validates the feasibility of the proposed antenna design methodology. The fabricated prototype shows good radiation performance and average gain at desired frequency bands. These features make the proposed antenna a good candidate for WLAN and X-band satellite communication applications.

ACKNOWLEDGMENT

This work was supported in part by the Zhejiang Provincial Natural Science Foundation of China under Grant No. LY12F04002 and National Natural Science Foundation of China under Grant No. 61340049 and No. 61671330.

REFERENCES

1. Gautam, A. K., L. Kumar, B. K. Kanaujia, and K. Rambabu, "Design of compact F-shaped slot triple-band antenna for WLAN/WiMAX applications," *IEEE Trans. Antennas Propag.*, Vol. 64, No. 3, 1101–1105, Mar. 2016.
2. Dong, X., Z. Liao, J. Xu, Q. Cai, and G. Liu, "Multiband and wideband planar antenna for WLAN and WiMAX applications," *Progress In Electromagnetics Research Letters*, Vol. 46, 101–106, 2014.
3. Rooyen, M. V., J. W. Odendaal, and J. Joubert, "High-gain directional antenna for WLAN and WiMAX applications," *IEEE Antennas Wireless Propag. Lett.*, Vol. 16, 286–289, 2017.
4. Yoon, J. H., and Y. C. Rhee, "Modified three-circular-ring monopole antenna for WiMAX/WLAN triple-band operations," *Microwave & Optical Technology Letters*, Vol. 56, No. 3, 625–631, 2014.
5. Sharma, A., P. Ranjan, and R. K. Gangwar, "Multiband cylindrical dielectric resonator antenna for WLAN/WiMAX application," *Electron. Lett.*, Vol. 53, No. 3, 132–134, Feb. 2017.
6. Abdulraheem, Y. I., G. A. Oguntala, A. S. Abdullah, H. J. Mohammed, R. A. Ali, R. A. Abd-Alhameed, and J. M. Noras, "Design of frequency reconfigurable multiband compact antenna using two PIN diodes for WLAN/WiMAX applications," *IET Microwaves, Antennas & Propag.*, Vol. 11, No. 8, 1098–1105, May 2017.
7. Chen, S., M. Fang, D. Dong, M. Han, and G. Liu, "Compact multiband antenna for GPS/WiMAX/WLAN applications," *Microwave and Optical Technology Letters*, Vol. 57, No. 8, 1769–1773, Aug. 2015.
8. Cui, Y. H., L. Yang, B. Y. Liu, and R. L. Li, "Multiband planar antenna for LTE/GSM/UMTS and WLAN/WiMAX handsets," *IET Microw. Antennas Propag.*, Vol. 10, No. 5, 502–506, 2016.
9. Liu, G., M. Fang, R. Zhi, J. Bai, and Z. Zeng, "Compact CPW-fed multiband antenna for TD-LTE/WLAN/WiMAX applications," *Progress In Electromagnetics Research Letters*, Vol. 65, 9–14, 2017.
10. Pandeeswari, R., "Complimentary split ring resonator inspired meandered CPW-fed monopole antenna for multiband operation," *Progress In Electromagnetics Research C*, Vol. 80, 13–20, 2018.